

A Numerical and Experimental Evaluation of the HP Litzcage for Human Head MRI at 3T

Jatin Kulkarni, John P. Staab, George Entzminger, Chunjiang Xiao, Nathan Laws, and F. David Doty
Doty Scientific, Columbia, SC

Abstract

Very recent advances in electromagnetic simulation tools now permit the degree of accuracy needed for quantitative, unambiguous evaluations and comparisons of high-field MRI RF coils, including the effects of the coupling networks, copper losses, capacitor losses, shield losses, and sample detuning. In this study, we numerically and experimentally evaluate three highly optimized homogeneous rf coils for human head MRI at 3T. The high-pass birdcage (HP-BC), the Balanced-High-Pass Litzcage (BHP-LC) and the Balanced-Low-Pass Litzcage (BLP-LC) are evaluated at 3T. All the coils are highly optimized and include external rf shields, several loads, and matching networks. A four-point-drive network is presented that provides a substantial advantage in maintaining coil symmetry over a wide tuning range. Experimental measurements, using both MRI and bench-top methods, validate the accuracy of the numerical simulations over a wide range of conditions.

Introduction

While many simulations of homogeneous rf resonators have been presented by various authors, most papers have focused on a single type of coil. The different methods and emphases of the various authors and different useful sample volumes of different coils make it difficult to compare the advantages and disadvantages of the various options. We attempt to objectively identify the advantages and the disadvantages of these coils with the goal of helping to assist the user in making more informed decisions on rf coil choices. Our use of a consistent method makes it easier to quantitatively compare different coils.

Our observations suggest that coils of a given type but different builders differ mostly in the coupling methods employed. As a result, the difference between a "good coil" and an inferior coil often can be traced to the coupling methods, and it is not uncommon for the losses associated with coupling details to exceed 15%, or for the coil's homogeneity to be very poor because of the coupling methods under some conditions of interest. We discuss the limitations of several coupling methods, and we describe methods that have proven effective in maintaining coil symmetry and matching over a wide range of loading conditions.

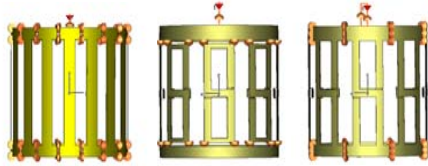


Figure 1 (a) 16-rung HP-BC, (b) 8-section Doty BLP-LC, (c) 8-section Doty BHP-LC. (In all three coils, some parts have been hidden for better clarity.)

The Coil Structures

All of the coils are fabricated from 0.06 mm copper foil (~10 skin depths at 128 MHz) on teflon substrate 0.5 mm thick and mounted on the outside of a lucite coilform which is 4 mm thick. The coil diameter is 280 mm and the external shield diameter is 336 mm. The end-rung width on the port end is 31.5 mm wide, whereas the end-rung width on the other end is 24.5 mm wide, and the inside distance between the end rings is 222 mm.

Our implementation of the 16-rung HP-BC is illustrated in **Figure 1 (a)** as simulated but with the shield, sample, sample container, coil form, and a few other details hidden for better clarity. The lumped capacitors are represented in the CST software graphically by chamfered disks. The Doty Balanced-Low-Pass LitzCage (D-BLP-LC), depicted in **Figure 1 (b)**, has insulated crossovers at the centers of the parallel rungs which keep the currents in the two rungs within each pair equal (this improves homogeneity considerably for some loads). Finally, **Figure 1 (c)** illustrates the Doty Balanced-High-Pass LitzCage (D-BHP-LC).

Some of the experimental data are summarized in **Table 1** for linear polarization with single-port drive. Note that for consistency with recent trends we are now reporting the matched Q of the resonator (with the sample and all losses), Q_L , which is half the isolated Q, Q_0 , that has more often been used in NMR SNR analyses. From the S_{11} (normalized reflected power) magnitude response,

$$Q_L = f_0 / \delta f \quad (2)$$

where δf is the width of the S_{11} peak at magnitude $S_{11} = (1 + S_{10}^2)^{1/2}$, where S_{10} is the magnitude of S_{11} at f_0 .

The Software, CST MWS 5.0

We carried out preliminary evaluations of three commercial electromagnetic simulation tools before concluding that CST MWS 4.2 had a number of advantages for our mix of rf problems, which includes small-animal MRI rf coils, solids NMR spectroscopy rf coils, high-resolution NMR spectroscopy sample coils, and high-field MRI head coils. We also found its geometry construction tools and interface to be much more powerful and much easier to use.

This CST code is based on a discretized solution of the integral formulation of Maxwell's equations; hence, the method is referred to as Finite Integration Technique (FIT). To solve these equations, a finite calculation domain is defined enclosing the application problem. A structured Cartesian mesh is created for half of the field equations (**E** and **B**), and a second Cartesian mesh, offset by half the element size in each direction from the first mesh, is created for the other half of the field equations (**H** and **D**). The use of two, offset meshes in this way greatly reduces discretization errors.

In this poster, we report primarily experimental validations of the software on the head-sized BHP-LC and BLP-LC under linear excitation, though we have also found similar, remarkable agreement with experiments for the very small solenoids and cross-coils (4-10 mm diameter) used in our solids NMR MAS probes.

Finally, we note that significant weaknesses of the software include the quality of the documentation and the technical guidance. These limitations can lead to a much longer learning curve than would initially be expected from simple test cases. However, when certain essential (but poorly documented) settings, options, methods, nomenclature, and techniques are properly understood, the software displays impressive versatility, power, and accuracy. Another current weakness is the newly included subgridding capability which is not yet compatible with our models. This is to be addressed within a few months and should permit much faster runs.

Circuit models and balanced matching networks

To simplify the amount of effort in this comparative coil study, we have limited our simulations and experiments to linear polarization, even though the coils are all directly compatible with circular polarization (CP) and the CST code easily accommodates CP drive. An rf circuit model is shown in **Figure 2** for the 8-section BHP-LC coil. It is somewhat better than one previously used in that the rungs are represented by a short transmission line at each end (TRL) with balanced couplings (C_{bc}) between adjacent rungs. Most of the losses are represented by appropriate attenuation coefficients in the TRLs and series resistances (R_{bc}) in the end ring segments (L_{bc}) and tuning capacitors (C_{bc}), but some appears explicitly as small series resistances R_s in series with the end-rung stray capacitances C_s .

For CP operation, coil symmetry is quite critical (at least for small coils) and sample detuning often exceeds the useful range of simple approaches – such as simply duplicating the input and balancing circuitry shown in **Figure 2** on the orthogonal plane (i.e., at nodes 25 and 65) for the second channel. Considerable improvement in coil symmetry and channel isolation is obtained by using a 4-point drive method. A simple method of doing such is to connect a low-loss half-wavelength transmission line between nodes 5 and 45 and another between nodes 25 and 65. This sometimes brings in additional common modes near the homogeneous modes, but small inductors from the center points (quarter-wavelength points) to ground on these phasing lines generally solve such problem.

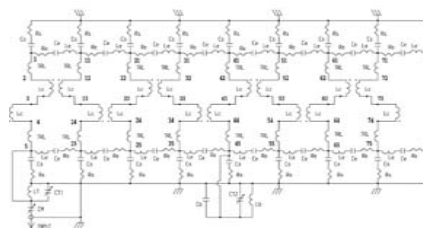


Figure 2 A BHP-LC rf circuit model with input and balancing networks that permits good agreement with experiments for $f < 20$ MHz-m, where d is the coil diameter.

Results and Discussion

The preliminary experimental validations showed the CST code to give excellent accuracy for Q_L and the mode frequencies for several 10 cm coils similar to birdcages. Our efforts started with a 205 MHz Crozier-Highpass-Birdcage with a slotted shield, as depicted in **Figure 3 (a)**. We later used a solid shield, shown in **Figure 3 (b)**, which led to a minor predictable shift in frequency but a considerable reduction in simulation time. We have persisted with the solid shield in subsequent simulations of the head coils, as described earlier under Structures.

Figure 4 shows the main homogeneous mode at 128.9 MHz for the D-BHP-LC with a 30 m cylindrical load, as obtained from CST MWS 5.0. The experiments showed modes within about 2% of those predicted by CST MWS 5.0 for several of the carefully executed experiments. Obtaining this level of accuracy for the unloaded case requires some extra mesh refinement beyond default conditions near the inside edges of the rings, and, in our litzcages, near the central crossovers. The total number of mesh cells is then around 200K. Achieving high accuracy with an aqueous sample also requires additional mesh refinement near the edges of the sample (both inside and outside of the sample boundaries), and this brings the total number of mesh cells to over 300K, though it could probably be reduced somewhat with more effort. **Figure 5** shows a view of the mesh, and **Figure 6** presents a view of the current density. Mode frequencies may be obtained with good accuracy (a few percent) within a few hours on a 3.2 GHz P-IV, but run times of 10-20 hours are currently needed for good accuracy on B1, QLC, and S11.

These coils were excited by a single port and hence we see the results of linear polarization. The new version, CST MWS 5.0, provides a feature to implement circular polarization, but we are still working on a macro to calculate the time-averaged fields, which we anticipate will agree well with MRI experiments and Tropp's recent analysis of central brightening.

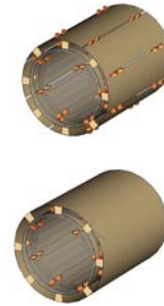


Figure 3 Crozier HP-BC with (a) slotted shield and (b) solid shield

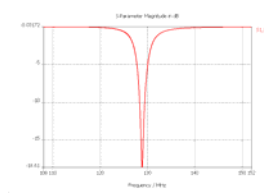


Figure 4 S11 in dB showing the homogeneous mode at 128.9 MHz for the D-BHP-LC with a 30m cylindrical load.

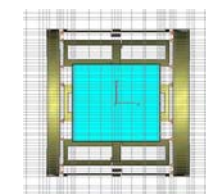


Figure 5 Mesh View of the Doty BLP-LC with a 30m cylindrical load showing the denser mesh lines near the crossovers and the end rings.

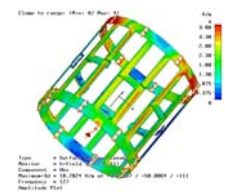


Figure 6 Current Density on the surface of the D-BHP-LC with a 30m cylindrical load (hidden in this figure).

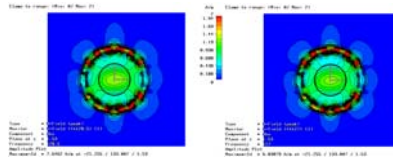


Figure 7 Absolute H field plot for linear polarization in the center of the D-BHP-LC coil with a 30 m cylindrical load (a) with inductor Lt (left) and (b) without inductor Lt (right).

With small coils, we have found it important to minimize the perturbation to the coil's symmetry from the matching capacitor by using an inductor Lt from the feed point to ground that tunes out the effects of the matching capacitor. An interesting observation from these simulations was that the effect of Lt is negligible for head-sized loads at 3T. For heavily loaded cases, where the sample dielectric resonance is dominating, asymmetries in the coil have relatively little effect. This is also in agreement with Tropp's recent seminal analysis, which essentially says about all the coil can do for large samples at high fields is determine the size of the excited region. The homogeneity and S/N are then determined almost totally by the sample. **Figure 7** gives a graphical representation of the H field (linear polarization) in a D-BHP-LC coil with a 30 m cylindrical load, clearly showing that the presence of Lt does not improve the homogeneity in this case.

Table 1 shows some experimental data for several coils tested. **Table 2** summarizes some results from CST MWS 5.0 for these cases, including central B_1 in μT for 1 W excitation. The previously reported MRI results at Penn State (Michael Smith, et al, http://www.dotynmr.com/mri/mri_headrfg.htm) yielded a mean central pi pulse of 49 W CP for a 3 mm Gaussian pulse on a human head with the brain centered in the coil. This is equivalent to a peak field of 0.092 G. Hence, 1 W CP would generate a central field of 1.3 μT or 1.03 A/m. This is, as expected, between the simulation values for our small and medium loads. (Inserting the head fully into the coil results in a considerably greater load.) The relatively large errors in QL under some conditions are not well understood, but are believed to be largely a result of incomplete treatment of some radiation boundaries and matching details. We note that small coils often show agreement between experiments and simulations within a few percent on Q_L using CST MWS software. It is very interesting to observe that the field with the 30 m saline load is twice that for the unloaded case, though Q_L is about 10 times larger for the unloaded case.

Expt. #	Coil Type	d mm	Sample	m_1 MHz	m_2 MHz	Q_L @ m_1	
1	D-BHP-LC	284	None	211	128.8	97	258
2	"	"	S	211	127.6	97	45.9
3	"	"	M	211	127.7	97	36.3
4	D-BLP-LC	284	None	212.24	131.65	118.19	136
5	"	"	S	212.97	126.41	-	32.9
6	"	"	M	212.57	127.42	94.52	20.6

Sample Load Types:
Small (S)- Cylinder of diameter 150 mm, length 170 mm, centered, salinity=30mM
Medium (M)- Cylinder of diameter 150 mm, length 170 mm, centered, salinity=100mM.

Expt. #	Coil Type	d mm	Sample	m_1 MHz	Q_L @ m_1	B_1 μT	m_1 % Error	Q_L % Error
1	D-BHP-LC	284	None	129.05	430	0.87	0.2	67
2	"	"	S	128.9	37	1.65	1	19
3	"	"	M	130.17	28.5	0.81	1.9	21.5
4	D-BLP-LC	284	None	129.68	259.3	0.65	1.5	90
5	"	"	S	124.7	49.8	1.58	1.3	51
6	"	"	M	126.63	32.8	0.8	0.6	60

Conclusions

The remarkable accuracy of the CST MWS 5.0 code in predicting the mode frequencies and B1 from a physically accurate model of the coil provides a very high level of confidence in its calculated fields and rf efficiencies – hence, S/N. For very light loads, the Litzcage often shows better B1 homogeneity than the 16-rung HP-BC coil. The shift in frequency due to sample loading effects is lower in the case of D-BHP-LC. The simulations show a barely discernable advantage in S/N for the BHP-LC, but its advantage in tunability is significant. Our results thus far agree completely with Tropp's recent analysis which indicates there can be no significant difference in S/N between different homogeneous head coils if their effective sample volumes are similar. More related experimental and numerical studies are planned for a variety of coil geometries and loads in the coming months. These will also include head and knee coils at higher frequencies (4 T and 7 T) and a hybrid (or Band-Pass) model.

References:

- F. D. Doty, G. Entzminger Jr, and C. D. Hauck, "Error-Tolerant RF Litz Coils for NMR/MRI", JMR 140:17-31, 1999.
- James Tropp, "Image Brightening in Samples of High Dielectric Constant", Journ. of Magn. Reson., 167, 12-24, 2004.

Acknowledgements: This work supported by R44 EB000445-02